

Calculation of high-order cumulants with canonical ensemble method in lattice QCD

Atsushi Nakamura

RCNP, Osaka University, Osaka567-0047, Japan

Nishina Center, RIKEN, Wako, Saitama 351-0198, Japan

School of Biomedicine, Far Eastern Federal University, Vladivostok, 690950 Russia

E-mail: atsushi@rcnp.osaka-u.ac.jp

Shotaro Oka

Institute of Theoretical Physics, Department of Physics, Rikkyo University

Toshima-ku, Tokyo 171-8501, Japan

E-mail: okasho-hato@rikkyo.ac.jp

Asobu Suzuki*

Graduate School of Pure and Applied Sciences, University of Tsukuba

Tsukuba, Ibaraki 305-8571, Japan

E-mail: suzuki@het.ph.tsukuba.ac.jp

Yusuke Taniguchi

Graduate School of Pure and Applied Sciences, University of Tsukuba

Tsukuba, Ibaraki 305-8571, Japan

E-mail: taniguchi@het.ph.tsukuba.ac.jp

High-order cumulants are quantities characterizing the probability distribution and have a lot of physical information. Baryon number cumulants are measured experimentally and show an indication of the confinement/deconfinement phase transition. We focus on quark number cumulants which are related with baryon number cumulants. However, it is difficult to calculate quark number cumulants in finite density lattice QCD because of the sign problem. In the present study we realize a calculation of quark number cumulants beyond $\mu/T \sim 1$ with the canonical approach in heavy quark region. Also, we study a finite density phase transition from a behavior of high-order cumulants.

The 33rd International Symposium on Lattice Field Theory

14 -18 July 2015

Kobe International Conference Center, Kobe, Japan

*Speaker.

1. Introduction

Finite density QCD has various phase structures, however a numerical simulation of them is quite difficult because of the sign problem. There are a lot of theoretical developments to attack the QCD phase diagram, and the canonical approach is well known as a candidate of it. In the present study, we especially focus on quark number cumulants and calculate them with the canonical approach. Because, experiments [1] show a deviation from Hadron Resonance gas model in the vicinity of the central collision energy 20GeV, and this behavior indicate the confinement/deconfinement phase transition. Moreover, it is easy to compare the numerical results with values of Hadron Resonance gas model and Quark Gluon gas model. Lattice calculation is very convenient tool in QCD, however, it is hard to understand the meaning of it without models or experiments. In this meaning, calculations of quark number cumulants are good tests to investigate how the canonical approach is helpful in finite density lattice QCD.

2. Calculation of quark number cumulants

In this section, we see a computational method of quark number cumulants in the present study. Since the sign problem makes it difficult to perform a numerical calculation of them, we used the canonical approach [2] combining with the winding number expansion method[3]. The canonical approach tells us a relation of the canonical partition function and the grand canonical one, and the winding number expansion method tells us a chemical potential dependence of a determinant of the Dirac operator. Quark number cumulants $\langle \hat{N}^k \rangle_c$ are defined through quark number moments $\langle \hat{N}^k \rangle$, which are given as follows.

$$\begin{aligned} \langle \hat{N}^k \rangle &= \frac{\partial^k}{\partial \left(\frac{\mu}{T}\right)^k} Z_{G.C.}(\mu) \\ &= \frac{1}{Z_{G.C.}(\mu)} \sum_N N^k Z_{can.}(N) e^{\frac{\mu}{T}N} \end{aligned} \quad (2.1)$$

In the first line we used the fugacity expansion of the grand canonical partition function $Z_{G.C.}$.

$$Z_{G.C.}(T, \mu; V) = \sum_N e^{\frac{\mu}{T}N} Z_{can.}(T; V, N) \quad (2.2)$$

It is natural to use the canonical approach to get quark number moments, because what we want to calculate is the canonical partition function. The canonical approach give us the inverse relationship of the fugacity expansion, which is a Fourier transformation of the grand canonical partition function.

$$Z_{can.}(T; V, N) = \frac{1}{2\pi} \int_{-\pi}^{\pi} d\frac{\mu}{T} Z_{G.C.}(T, i\mu; V) e^{-i\frac{\mu}{T}N} \quad (2.3)$$

Moreover, we can see that the canonical partition function is a more manageable observable compared with the grand canonical one in finite density lattice QCD. This property comes from the γ_5 hermiticity of the Dirac operator for a pure imaginary chemical potential

$$\gamma_5 D(i\mu) \gamma_5 = D^\dagger(i\mu), \text{ for } \mu \in \mathcal{R}. \quad (2.4)$$

When we consider 2-flavor case, the sign problem do not appear from the Dirac operator, because the determinant of it is real and positive. We used the winding number expansion method to calculate the determinant of the Dirac operator. The winding number expansion method gives the determinant of the Dirac operator as follows.

$$\det D(\mu) = e^{Tr\{\log(1-\kappa Q)\}} = \exp\left(-\sum_{n=1}^{\infty} \frac{\kappa^n}{n} Tr\{Q^n\}\right) = \exp\left(\sum_k W_k e^{\frac{\mu}{T}k}\right), \quad (2.5)$$

where we defined

$$\begin{aligned} Q &= \sum_{i=1}^3 \left(Q_i^{(+)} + Q_i^{(-)} \right) + e^{\mu} Q_4^{(+)} + e^{-\mu} Q_4^{(-)} \\ Q_{\mu}^{(+)}(x, y) &:= (1 - \gamma_{\mu}) U_{\mu}(x) \delta_{x, y - \hat{\mu}} \\ Q_{\mu}^{(-)}(x, y) &:= (1 + \gamma_{\mu}) U_{\mu}^{\dagger}(x - \hat{\mu}) \delta_{x, y + \hat{\mu}}, \mu = 1 \cdots 4. \end{aligned} \quad (2.6)$$

Coefficients $\{W_k\}_k$ does not depend on a chemical potential and subscript k means winding number of quark loop in the temporal direction. Therefore, once we get them it is easy to calculate the determinant for an arbitrary chemical potential. However, we must restrict quark mass to heavy as $m_{\pi}/m_{\rho} \sim 0.8$ because the winding number expansion method makes use of the hopping parameter expansion method.

In the present study, we also use the reweighting technique¹.

$$Z_{can.}(T; V, N) = \frac{1}{2\pi} \int_{-\pi}^{\pi} d\frac{\mu}{T} \int \mathcal{D}U \frac{\det D(i\mu)}{\det D(0)} e^{-i\frac{\mu}{T}N} \det D(0) e^{-S_g} \quad (2.7)$$

We can regard $\det D(\mu = 0) e^{-S_g}$ as a probability of the Monte Carlo simulation and the other part as a observable. Now we can calculate the canonical partition function, thus quark number cumulants. However, as we will see later we cannot avoid the sign problem especially at low temperature.

3. Lattice setup

In this study we used the Iwasaki gauge action and the 2-flavor Wilson-Clover fermion action to perform the Monte Carlo simulation. The lattice volume is $8^3 \times 4$, and the other parameters (β, κ, C_{SW}) is listed on table 1. Temperature is related to coupling β and our parameter set covers a wide range of temperature from $T/T_c = 0.644$ to $T/T_c = 3.45$. To perform the winding number expansion method we used the hopping parameter expansion method and the maximum order of it is taken to 480.

¹To perform the numerical Fourier transformation we used the multiprecision calculations. This is suggested in [3][4].

β	κ	C_{SW}	T/T_c	m_π/m_ρ
0.9	0.137	1.1	0.644	0.8978(55)
1.1	0.133	1.1	0.673	0.9038(56)
1.3	0.133	1.1	0.706	0.8770(52)
1.4	0.132	1.1	NA	NA
1.5	0.131	1.1	0.813	0.8486(58)
1.6	0.130	1.1	NA	NA
1.7	0.129	1.1	1.00	0.770(13)
1.8	0.126	1.1	NA	NA
1.9	0.125	1.1	1.68	0.714(15)
2.1	0.122	1.1	3.45	0.836(47)

Table 1: Parameters used in this study. We changed β from the confined phase to the deconfined phase and made κ small to perform the winding number expansion.

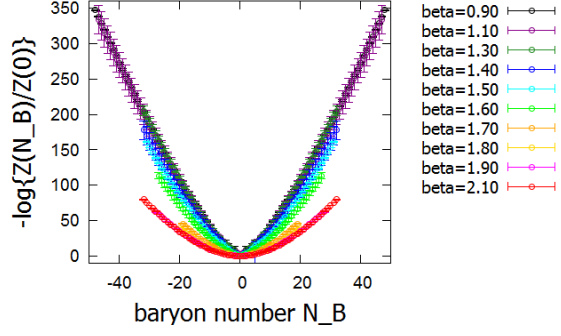


Figure 1: Numerical results of the normalized canonical partition function $-\log(Z_{can.}(N_B)/Z_{can.}(0))$. Horizontal axis shows the baryon number, three times of quark number $N_B = 3N$. The difference of colors corresponds to the difference of β .

4. Numerical results

It is useful to consider a ratio of quark number cumulants because the expressions of it become simple in the free gas models. We calculated variance $\langle \hat{N}^2 \rangle_c / \langle \hat{N}^1 \rangle_c$, skewness $\langle \hat{N}^3 \rangle_c / \langle \hat{N}^1 \rangle_c$ and kurtosis $\langle \hat{N}^4 \rangle_c / \langle \hat{N}^2 \rangle_c$ of quark number cumulants, and compared the numerical results with the model results. In Hadron Resonance gas model they are given by

$$\frac{\langle \hat{N}^2 \rangle_c}{\langle \hat{N}^1 \rangle_c} = 3 \coth\left(3\frac{\mu}{T}\right) = 3 \coth\left(\frac{\mu_B}{T}\right) \quad (4.1)$$

$$\frac{\langle \hat{N}^3 \rangle_c}{\langle \hat{N}^1 \rangle_c} = \frac{\langle \hat{N}^4 \rangle_c}{\langle \hat{N}^2 \rangle_c} = 9, \quad (4.2)$$

and in Quark Gluon gas model

$$\frac{\langle \hat{N}^2 \rangle_c}{\langle \hat{N}^1 \rangle_c} = \frac{\left\{1 + \frac{3}{\pi^2} \left(\frac{\mu}{T}\right)^2\right\}}{\left\{\frac{\mu}{T} + \frac{1}{\pi^2} \left(\frac{\mu}{T}\right)^3\right\}} \quad (4.3)$$

$$\frac{\langle \hat{N}^3 \rangle_c}{\langle \hat{N}^1 \rangle_c} = \frac{\frac{6}{\pi^2} \frac{\mu}{T}}{\left\{\frac{\mu}{T} + \frac{1}{\pi^2} \left(\frac{\mu}{T}\right)^3\right\}} \quad (4.4)$$

$$\frac{\langle \hat{N}^4 \rangle_c}{\langle \hat{N}^2 \rangle_c} = \frac{\frac{6}{\pi^2}}{\left\{1 + \frac{3}{\pi^2} \left(\frac{\mu}{T}\right)^2\right\}}. \quad (4.5)$$

At first we calculated the canonical partition function as in figure 1. However, we cannot evaluate the canonical partition function for large quark number. When we consider the concavity of a free energy with respect to quark number, we can show monotonic decrement of $Z_{can.}(N+3)/Z_{can.}(N)$.

$$\log(Z_{can.}(N+3)) \geq \frac{1}{2} \{\log(Z_{can.}(N)) + \log(Z_{can.}(N+6))\}$$

$$\begin{aligned}
&= \log \left(\sqrt{Z_{can.}(N)Z_{can.}(N+6)} \right) \\
&\Leftrightarrow \frac{Z_{can.}(N+3)}{Z_{can.}(N)} - \frac{Z_{can.}(N+6)}{Z_{can.}(N+3)} \geq 0
\end{aligned} \tag{4.6}$$

We claimed this condition as a necessary condition. Moreover, we can get consistent result with the direct computation of the determinant [5] within error bars under this condition. Figure 1 shows the canonical partition function in the application range of the winding number expansion method. We constructed quark number cumulants from this result. We set the canonical partition function when it does not satisfy the condition (4.6).

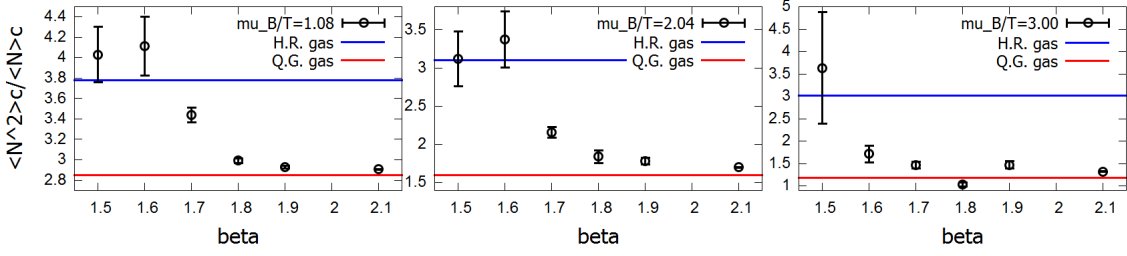


Figure 2: Variance as a function of β .

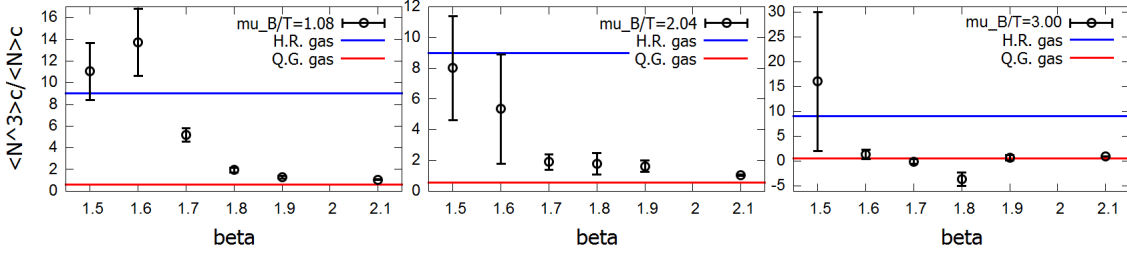


Figure 3: Skewness as a function of β .

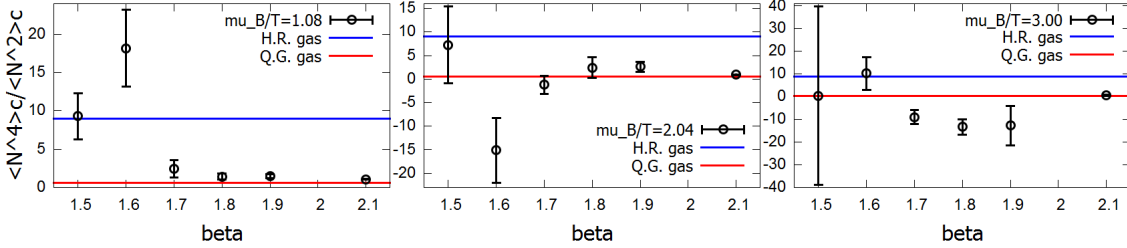


Figure 4: Kurtosis as a function of β .

Figure 2 shows variance, Figure 3 shows skewness and Figure 4 shows kurtosis as a function of β . Each points show numerical results, the blue solid line shows Hadron Resonance gas model results and the red solid line shows Quark Gluon gas model results. We fix μ_B/T to (1.08, 2.04, 3.00) for the each figures. Because of the sign problem there are large error bars at low temperature, on the other hand, at high temperature the sign problem is under control.

Moreover, we can see a transition from H.R. gas to Q.G. gas. For the variance. When we increase the chemical potential, the place of the deviation from H.R. gas decrease. This behavior is consistent with the previous work [6] qualitatively. Skewness shows same behavior with the variance. Kurtosis shows unique behavior at $\mu_B/T = 2.04$. The numerical results oscillate around $\beta = 1.6$,

kurtosis once takes a negative value around $\beta = 1.6$ and approaches to the Q.G. gas result. Since we can construct the observables with the fugacity expansion, it is easy to see them as a function of μ/T in the canonical approach. However, we have to take care about the effect of the truncation of the fugacity expansion, which makes an artificial phase transition. We estimated the place of the artificial transition μ_B^{cut}/T from the ratio test. In other words, when the observable is calculated by

$$\sum_{n=-N_{cut}}^{N_{cut}} O_n e^{\frac{\mu_B}{T}n}, O_n = \begin{cases} Z_{can.}(3n) & (\text{for } Z_{G.C.}) \\ (3n)^k Z_{can.}(3n) & (\text{for } \langle \hat{N}^k \rangle_c) \end{cases}, \quad (4.7)$$

we estimate the μ_B^{cut}/T from

$$\frac{O_{N_{cut}}}{O_{N_{cut}-1}} e^{\frac{\mu_B^{cut}}{T}} = 1. \quad (4.8)$$

In the following discussion numerical results are bounded by the condition(4.8). Thus, there is no need to take the artificial phase transition into account.

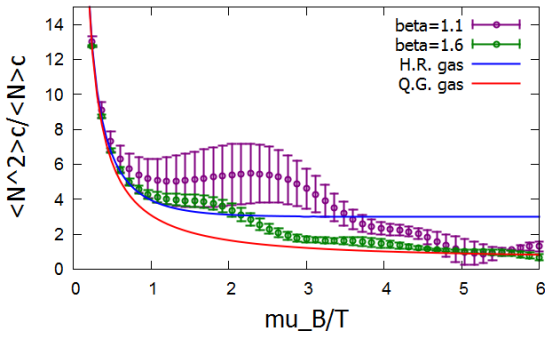


Figure 5: Variance at low temperature as a function of μ_B/T .

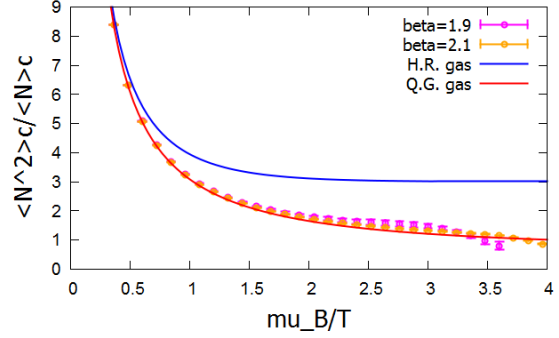


Figure 6: Variance at high temperature as a function of μ_B/T .

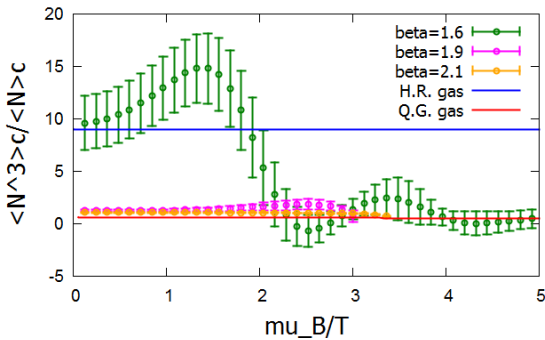


Figure 7: Skewness for $\beta = 1.6$ ($T < T_c$) as a function of μ_B/T .

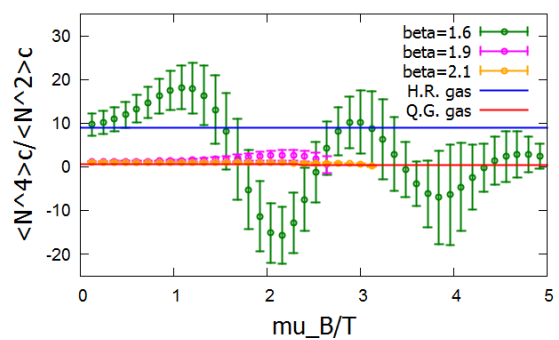


Figure 8: Kurtosis for $\beta = 1.6$ ($T < T_c$) as a function of μ_B/T .

Figure 5,6 show variance, Figure 7 shows skewness and Figure 8 shows kurtosis as a function of μ_B/T . The blue solid line express H.R. gas and the red solid line express Q.G. gas. In the present study we can evaluate skewness and kurtosis only for $\beta \geq 1.6$. From the results of variance and skewness, we can see a transition from H.R. gas to Q.G. gas at low temperature, and we do not see such a transition at high temperature. This behavior can be expected from the QCD phase diagram. Kurtosis shows a unique behavior at low temperature. The numerical result shows an oscillation around $\mu_B/T \sim 2$, which is located between H.R. gas region and Q.G. gas region. Therefore, we can expect that this oscillation indicate the phase transition.

5. Conclusion

In this study we calculated quark number cumulants and compared them with the two free gas models. The present calculations are restricted in heavy quark region to use the winding number expansion method. The canonical approach works well, and we can evaluate the cumulants beyond $\mu/T \sim 1$ even at low temperature. From the behavior of the variance and skewness we saw a Hadron Resonance gas to Quark Gluon gas transition. Kurtosis showed an oscillation between H.R. gas and Q.G. gas region at low temperature. Of course, we must study the volume dependence of the cumulants to discuss an order of the phase transition. However, since the sign problem makes the error bars so large at low temperature, there is a possibility to fail numerical simulations when we increase the lattice volume.

Acknowledgement

This work is done for Zn Collaboration. We would like to thank R. Fukuda and S. Sakai. This work is supported by the Large Scale Simulation Program No.14/15-19 (FY2014) of High Energy Accelerator Research Organization (KEK). This work is supported in part by Grants-in-Aid of the Ministry of Education (Nos. 26610072, 24340054, 22540265). This work is in part based on Bridge++ code (<http://suchix.kek.jp/bridge/Lattice-code/>).

References

- [1] STAR Collaboration, Phys. Rev. Lett. 113, 092301 (2014), arXiv:1402.1558 [nucl-ex].
- [2] A. Hasenfratz and D. Toussaint, Nucl. Phys. B 371, 539 (1992).
- [3] A. Li, A. Alexandru, K. F. Liu and X. Meng, Phys. Rev. D 82, 054502 (2010), arXiv:1005.4158 [hep-lat].
- [4] R. Fukuda, A. Nakamura, and S. Oka, arXiv:1504.06351 [hep-lat].
- [5] K. Nagata and A. Nakamura, Phys. Rev. D 82, 094027 (2010), arXiv:1009.2149.
- [6] C. Gattringer and H. P. Schadler, Phys. Rev. D 91, 074511 (2015), arXiv:1411.5133 [hep-lat].
- [7] A. Nakamura, S. Oka and Y. Taniguchi, arXiv:1504.04096 [hep-lat].
- [8] A. Nakamura, S. Oka and Y. Taniguchi, arXiv:1504.04471 [hep-lat].